

Electronic Supplementary Information

## Ferroelectric $\text{Hf}_{0.5}\text{Zr}_{0.5}\text{O}_2$ films with improved endurance obtained through low temperature epitaxial growth on seed layers

Tingfeng Song,<sup>a</sup> Romain Bachelet,<sup>b</sup> Guillaume Saint-Girons,<sup>b</sup> Ignasi Fina,<sup>a,\*</sup> Florencio Sánchez<sup>a,\*</sup>

<sup>a</sup> Institut de Ciència de Materials de Barcelona (ICMAB-CSIC), Campus UAB, Bellaterra 08193, Barcelona, Spain

<sup>b</sup> Univ. Lyon, Ecole Centrale de Lyon, INSA Lyon, Université Claude Bernard Lyon 1, CPE Lyon, CNRS, Institut des Nanotechnologies de Lyon - INL, UMR5270, 69134 Ecully, France.

\* ifina@icmab.es, fsanchez@icmab.es

### Figure S1 XRD Pole figures

Pole figures (top panels) and  $\phi$ -scans (bottom panels) around asymmetrical o-HZO(-111) and STO(111) reflections of the (a)  $T_s = 550\text{ }^\circ\text{C}$ , (b)  $T_s = 650\text{ }^\circ\text{C}$ , and (c)  $T_s = 800\text{ }^\circ\text{C}$  samples.

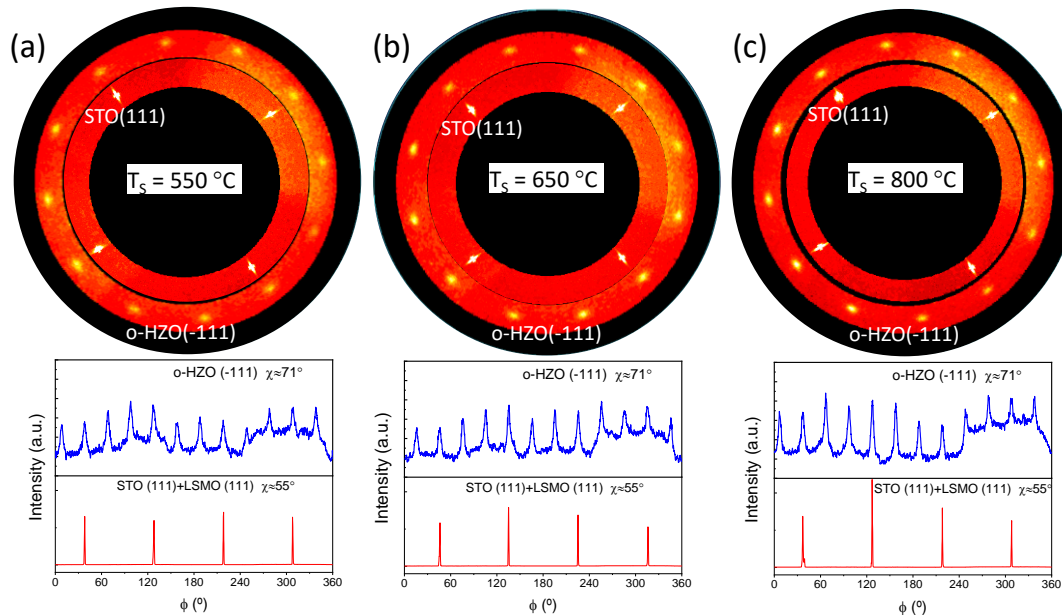


**Figure S2 XRD  $2\theta - \chi$  maps measured with 2D detector**

XRD  $2\theta - \chi$  maps measured around  $\chi = 0^\circ$  from  $2\theta = 20^\circ$  to  $50^\circ$ . The main reflections are indexed at the top. The asterisk mark the position of the m-HZO(-111) reflection in the low  $T_s$  films and a Laue fringe in the high  $T_s$  films.

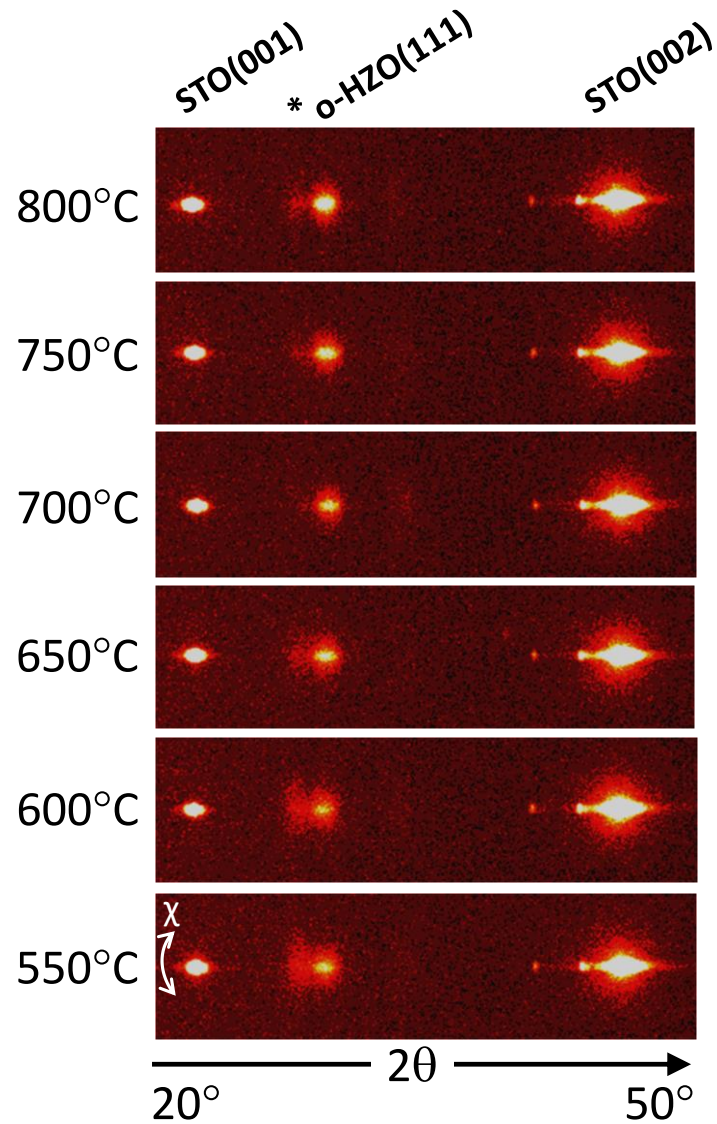


**Figure S3 Simulation of Laue fringes**

Figure S3 shows the XRD  $\theta$ - $2\theta$  scan of the HZO/LSMO/STO(001) samples. The patterns around the HZO(111) reflections are simulated according the dependence:

$$I(Q) = \left( \frac{\sin\left(\frac{QNc}{2}\right)}{\sin\left(\frac{Qc}{2}\right)} \right)^2$$

where  $Q = 4\pi\sin(\theta)/\lambda$  is the reciprocal space vector,  $N$  the number of unit cells along the out-of-plane direction and  $c$  the corresponding lattice parameter. The simulations (red curves) have been fitted supposing the  $Nc$  thickness indicated in each panel.

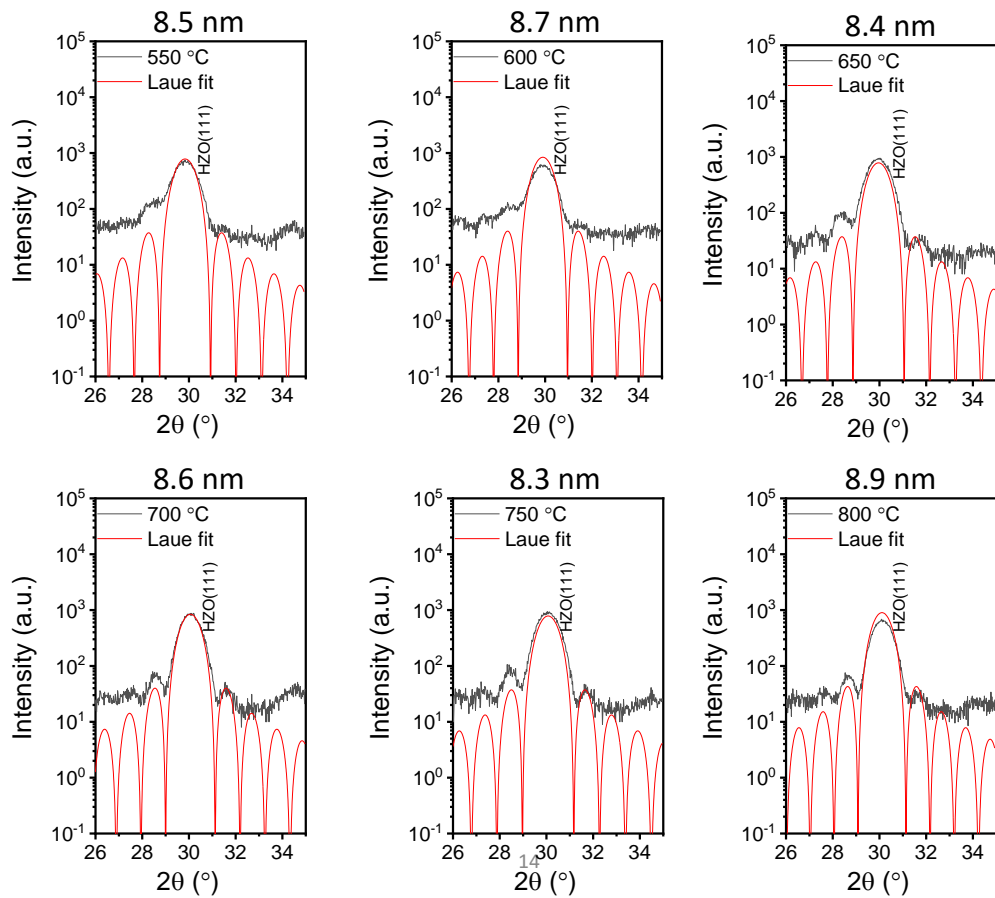


**Figure S4 XRD  $\theta$ - $2\theta$  scans of HZO films deposited on Si(001)**

XRD  $\theta$ - $2\theta$  scans of HZO films deposited on Si(001) at the temperature indicated on the right. Scans are shifted vertically for clarity. The enlarged  $2\theta$  region shown in the right panel was scanned with a longer acquisition time. The dashed vertical line marks the position of the peak in the  $T_s = 750$  °C sample.

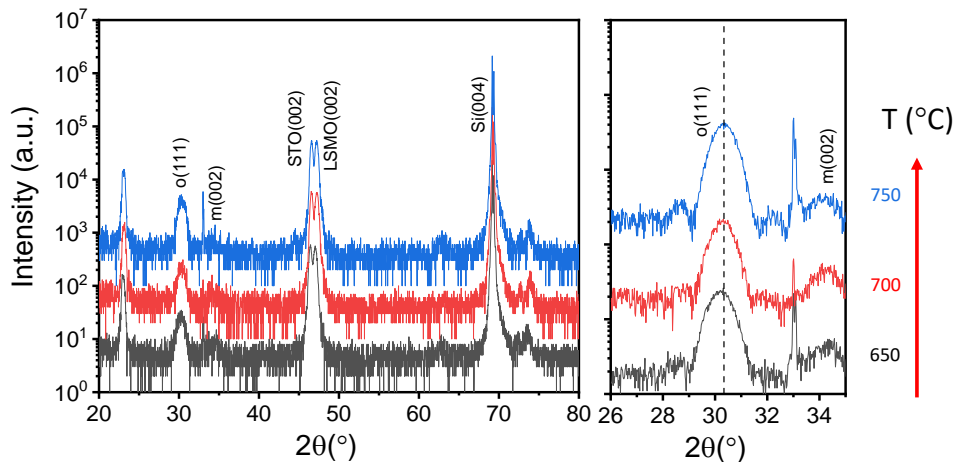


**Figure S5 Current-voltage loops measured in the HZO films deposited on STO(001)**

Current-voltage loops measured in the HZO films deposited on STO(001) at the temperature indicated in the bottom right. Polarization loops shown in Figure 3a were obtained by integration of these current - voltage loops.

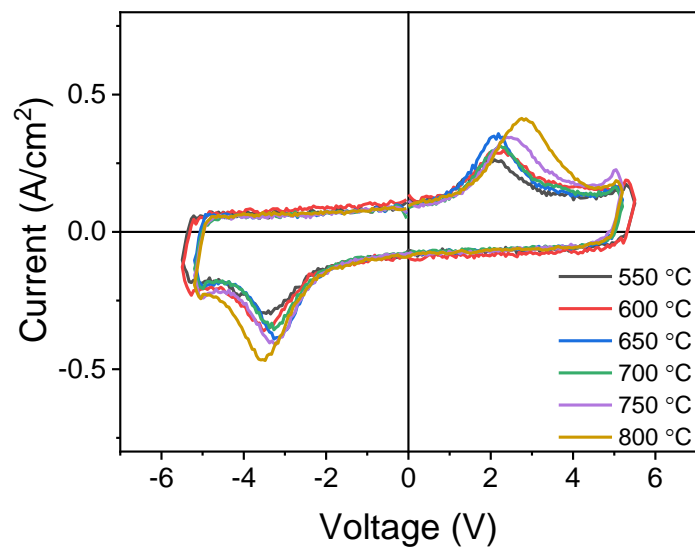


**Figure S6 Current - voltage and corresponding polarization - voltage loops of the HZO films deposited on Si(001)**

Current - voltage (a) and corresponding polarization - voltage (b) loops of the HZO films deposited on Si(001) at the temperature indicated in the bottom right.

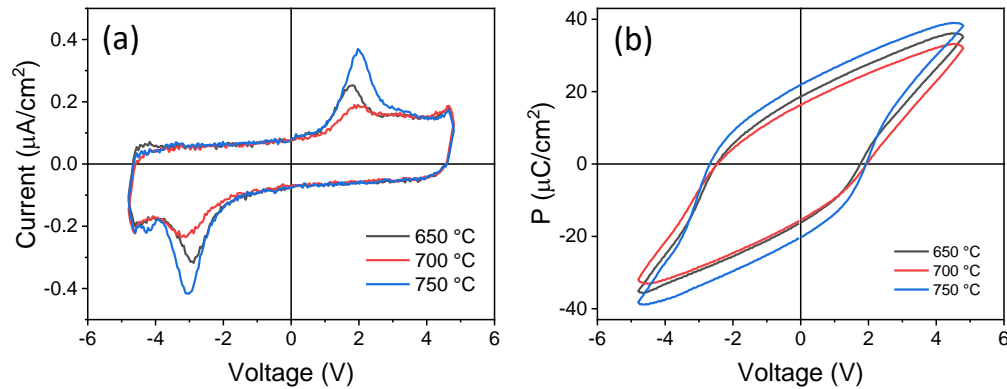


**Figure S7 PUND measurements**

In Figure S7(a), the PUND loops measured with 1 s delay time for all the studied samples are shown. Similar  $P_r$  values are obtained. In Figure S7(b), a comparison of the loops obtained with dynamic and PUND methods for a representative sample ( $T_s = 750$  °C) is shown. It can be observed that the coercive field is larger for the PUND loop. This results from the presence of the fluid imprint field<sup>1</sup>. The increase of coercive field does not allow to fully saturate the polarization of the sample at the used maximum applied electric field. Larger electric field results on device breakdown. In Figure S7(c), it can be observed that the  $P_r$  obtained using PUND is slightly less than those obtained by dynamic method. In both cases the trend is the same indicating that the decrease of polarization while decreasing  $T_s$  is small.

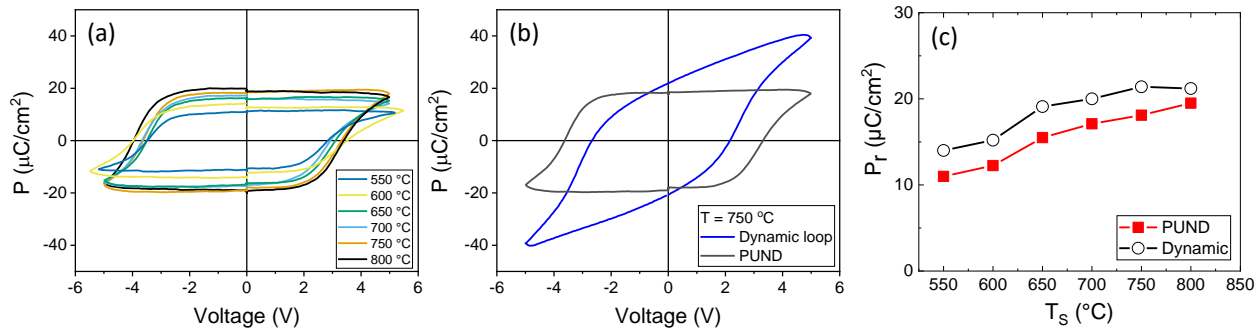


**Figure S8 Polarization – voltage loops measured in the pristine state and after the indicated number of cycles**

Polarization – voltage loops measured in the pristine state and after the indicated number of cycles (indicated at the bottom right in each panel) for films on STO(001) deposited at the temperature indicated in the top right of each panel. Loops are a selection of the measured to plot the endurance graphs shown in Figures 4 a-f.

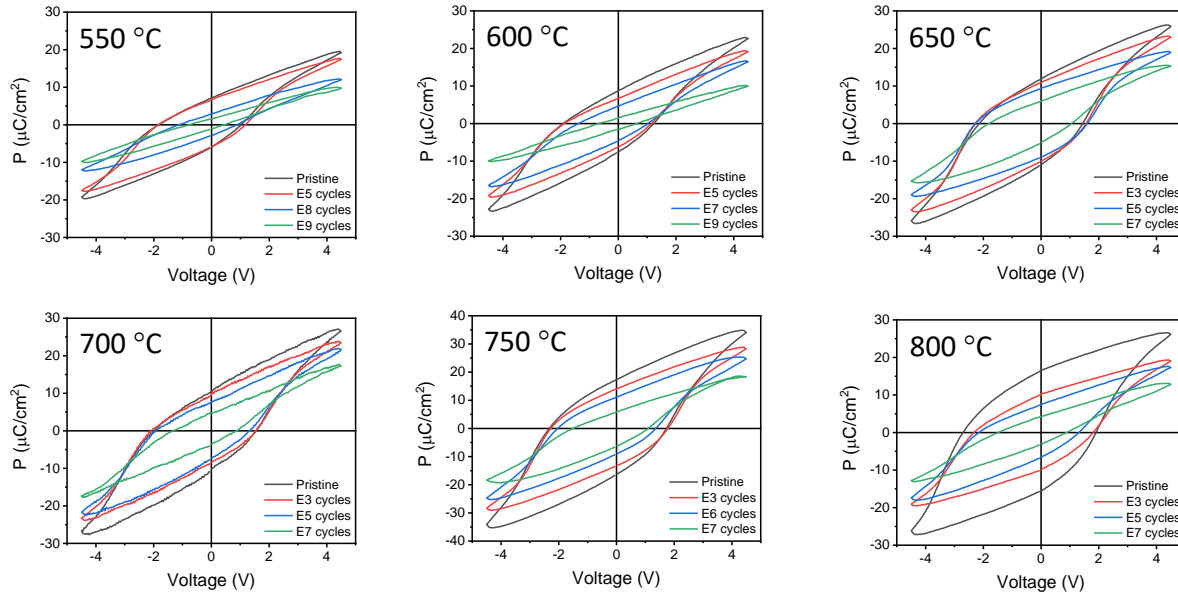


**Figure S9 Polarization retention measurements for films on STO(001)**

Polarization retention measurements at for positive (blue squares) and negative (red circles) poling of 4.5 V for films on STO(001) deposited at the temperature indicated in the top right of each panel. Lines are fits to  $P_r = P_0 \cdot t_d^{-n}$  equation.

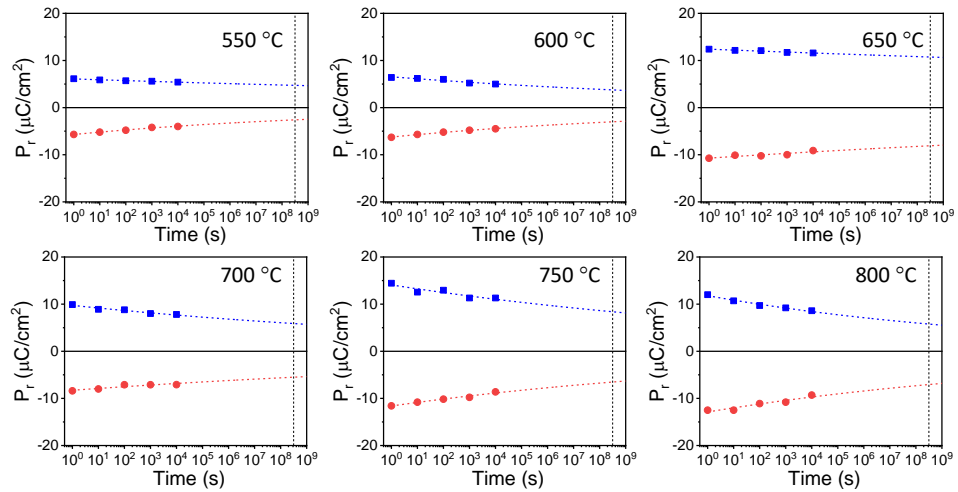
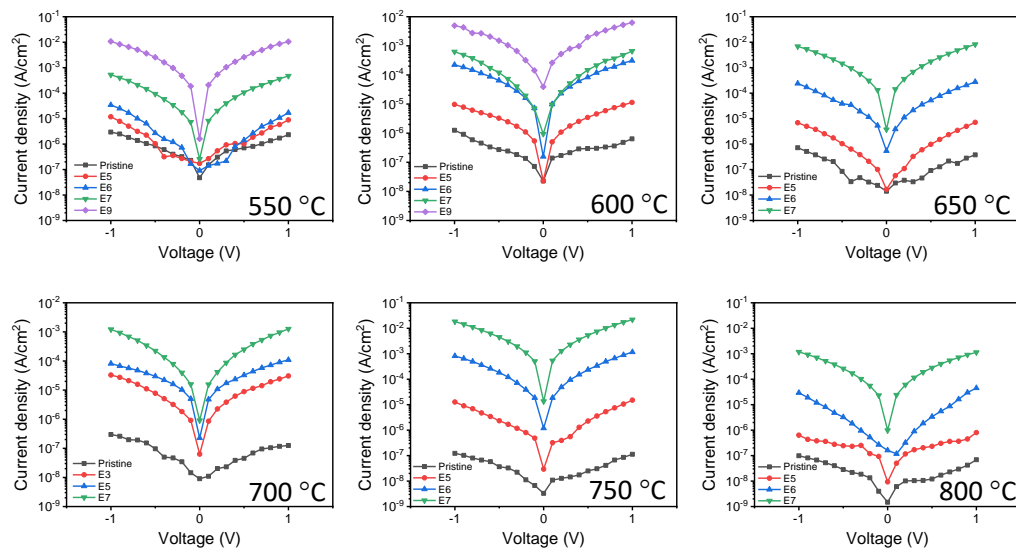


**Figure S10 Leakage current curves measured in the pristine state and after the indicated number of cycles**

Leakage current curves measured in the pristine state and after the indicated number of cycles (indicated at the bottom left in each panel) for films on STO(001) deposited at the temperature indicated in the bottom right of each panel. Figure 5 is plotted from leakage data at -1 and +1 V in these curves.



## Reference

- 1 P. Buragohain, A. Erickson, P. Kariuki, T. Mittmann, C. Richter, P. D. Lomenzo, H. Lu, T. Schenk, T. Mikolajick, U. Schroeder and A. Gruverman, *ACS Appl Mater Interfaces*, 2019, **11**, 35115–35121.